UNCONVENTIONAL APPLICATIONS OF A1040 MIRA TOMOGRAPH

M. Bellanova[1], M. Cucchi[2], R. Felicetti[3], F. Lo Monte[4]

[1]Dipartimento di Ingegneria Civile e Ambientale, Politecnico di Milano
Piazza Leonardo da Vinci, 32 - 20133 Milano
Tel.: +39 02 23994212 - Fax: +39 02 23994220 - email: mariagrazia.bellanova@polimi.it

[2] Laboratorio Prove Materiali, Politecnico di Milano
via Celoria 3, 20133 Milano
Tel.: +39 02 23994368 - Fax: +39 02 23994211 - email: marco.cucchi@polimi.it

[3]Dipartimento di Ingegneria Civile e Ambientale, Politecnico di Milano
Piazza Leonardo da Vinci, 32 - 20133 Milano
Tel.: +39 02 23994388 - Fax: +39 02 23994220 - email: roberto.felicetti@polimi.it

[4]Dipartimento di Ingegneria Civile e Ambientale, Politecnico di Milano
Piazza Leonardo da Vinci, 32 - 20133 Milano
Tel.: +39 02 23994379 - Fax: +39 02 23994220 - email: francesco.lo@polimi.it

Keywords: guided waves, SAFT, tomography, ultrasonic pulse echo

One of the most innovative tools available for ultrasonic imaging of concrete and stone elements is the A1040 MIRA tomograph, which was launched about 15 years ago by Acoustic Control Systems (Moscow, Russia). This instrument was devised to systematically implement the pulse-echo technique via a shear wave transducer array coupled to one side of the structure. Particularly interesting features are the spring-loaded dry point-contact sensors, the automatic implementation of tomographic B-scans via the Synthetic Aperture Focusing Technique and the availability of rough acquired data for customized post-processing.

Taking advantage of this last option, the authors started extending the use of this device to some specific problems beyond the bare localization of voids. One first example is the extraction of quantitative information about the magnitude and phase of pulses ensuing from detected reflectors. This allows a more objective judgment on the effectiveness of cement injections and duct grouting.

Another application is the assessment of surface damage due to fire exposure. Though pulse refraction due to steep velocity gradients makes focusing of images difficult, the decay of surface waves velocity can be easily detected from the onset of received pulses.

The last example deals with the implementation of the Guided Waves method to ancient wrought iron tie-rods including coarse welding defects. Here the adaptable point sensors proved to be very effective in coupling the instrument to the remarkably rough surface of the elements.

The discussion of these special applications will further promote the interest in this renowned diagnostic tool for Civil Structures.

1. INTRODUCTION

Acoustic methods are commonly used for the inspection of concrete structures, either in the sonic ($f < 20$ kHz) or ultrasonic ($f > 20$ kHz) frequency range. The most common use is the assessment of bulk velocity in order to estimate the average material quality. Other more advanced applications include evaluation of element thickness, detection of cracks and voids, location of coarse reinforcement and post-tensioning ducts, check of grout injections [1]. However several difficulties have to be tackled in this second case, since concrete is a heterogeneous material made of cement matrix, aggregates of assorted size and air pores. At every inherent interface (cement-aggregate or cement-pores) or other strong acoustic inhomogeneity, waves travelling thorough the medium are scattered, due to secondary reflections and refractions. This is the reason why significant structural noise and attenuation affect the results, especially at frequencies exceeding 100kHz [2]. Moreover, different wave types are triggered at the interfaces (mode conversion), each one characterized by a different propagation velocity. This translates into dispersion and distortion of the detected waves. For these reasons, the Ultrasonic Pulse Velocity method (UPV) keeps being the most popular among acoustic inspection methods. According to this technique, the assessment of the material response is based on transmitted pulses travelling along the path defined by the mutual position of distinct emitting (TX) and receiving (RX) probes. Since just the front edge is picked in the received signal, the Time Of Flight (TOF) is governed by straight propagation in the fastest mode (compression wave) and not affected by the cited disturbances.

As an alternative, impact-echo (IE) and pulse-echo (PE) methods can be used. They are based on detection of signals reflected by internal discontinuities back to the same location where a short mechanical pulse is triggered. In order to allow for multiple indications coming from different reflectors, the whole signal during an inclusive time window has to be analysed, bringing in the effects of scattering and dispersion.

Impact-echo is carried out on elements with regular shape, mostly slabs and walls of unknown thickness and possibly containing sizable voids or delamination cracks. In most cases the pulse is generated by a small impactor (steel ball or hammer) hitting the surface. Examination is based on frequency analysis of multiple reflections of waves occurring between the interface being detected and the external surface where the test is implemented. The resonance frequencies provide information about the depth of acoustic interfaces, with little influence of incoherent signal components due to structural noise.

On the contrary, pulse-echo is based on just the first reflection of the diagnostic pulse emitted by a piezoelectric transducer. More complex element geometry can be inspected provided that the test is repeated over a regular grid of measurement points [3]. This allows to discriminate and locate different reflectors, whose indications are overlapped in a single time domain signal (A-scan). Instruments fitted with sensor arrays or automated probe positioning systems are particularly suited to this kind of application [4].

Many imaging techniques have been developed in order to merge measurements into tomographic images while reducing the inherent structural noise. Among them, Synthetic Aperture Focusing Technique (SAFT) provides very effective results. The algorithm focuses signals reflected at any position in the tomographic image through a coherent superposition (time shift) based on the total geometrical distance travelled by each pulse [5]. Either linear or planar acquisition grids can be adopted which return two- and three-dimensional representations respectively.

2D SAFT images are sections orthogonal to the test surface (B-scan), while 3D SAFT outputs are displayed either as orthogonal or parallel sections through three-dimensional data field (B- and C-scans). SAF Technique allows also the reconstruction of the element boundaries (perfect reflectors), which may be taken as reference in the assessment of other reflectors strength. Moreover, structural noise and waves undergoing mode conversion are defocused leading to a reduction of disturbing signals.
Phase analysis in SAFT-reconstructed images can help to recognize different types of discontinuities [6]. Air to concrete interfaces entail complete reflection and phase reversal of pulses, while a partial reflection with the same phase occurs at the interface to materials of higher acoustic impedance than concrete (e.g. steel bars).
At present, the most viable tool for automated implementation of pulse-echo imaging in concrete elements is the A1040 MIRA tomograph by Acoustic Control System (Russia). Some interesting features of this device are recalled in the following, together with the procedure followed for raw waveform acquisition. Then, some alternative schemes for data processing are discussed in order to devise the possible extension of its use to specific applications which may take advantage of the built-in array of emitting/receiving sensors.

2. DEVICE CONCEPT AND FEATURES

The A1040 MIRA tomograph is an advanced multi-sensor ultrasonic device for concrete inspection based on the pulse-echo method. It has been developed about two decades ago by Acoustic Control System in collaboration with the Federal Institute for Material Research and Testing (BAM) in Germany. One key feature of this instrument is the array of 48 highly damped Dry Point Contact (DPC) transducers (Fig. 1). The sensors are loaded by independent springs, allowing to adapt on uneven and rough surfaces. They are also fitted with wear resistant ceramic contact tips, not requiring any coupling agent.
In the current version, the array is organized in 12 blocks of 4 transducers each. Every block operates as a single emitting/receiving broad-band shear-wave sensor (polarization plane along x-axis in Fig.1). Though the central frequency of the sensors is 50kHz, the emitted pulses may driven in the range between 25 and 85 kHz, thanks to high damping. Since the size of blocks in the polarization plane (90 mm) is larger than the wavelength in normal applications ($\approx$ 50 mm), a narrow divergence angle of the emitted pulses results in the same plane. On the contrary, the size is negligible along the array axis, which implies a broad divergence angle in the B-scan plane (y-axis in Fig. 1), and then the ability to inspect a significant width about the centre of the array (generally $\pm$175 mm).
The main advantage brought in by the adoption of shear waves is that they are not affected by mode conversion when reflected and they are characterized by shorter wavelengths (higher resolution) at a given frequency. On the other hand, narrow interfaces due to rebars and ducts can be detected just when they are oriented parallel to the polarization plane.
Concerning data acquisition, each transducer block acts in turn as receiver or emitter. According to the numbering convention shown in Fig. 1, the first block is set as receiver and the following ones work in turn as emitters (Fig. 2). Then the second block is set as receiver and, again, the following ones pulse in sequence. In summary 66 A-scan (2048 samples, 14 bit @ 1MHz) are collected in about 3 seconds and then processed in the form of a B scan along the y-axis. Acquired data are also made available in binary files for customized post processing. The main technical features of A1040 MIRA Tomograph are summarized in Table 1.

Fig. 1: device and its sensor array

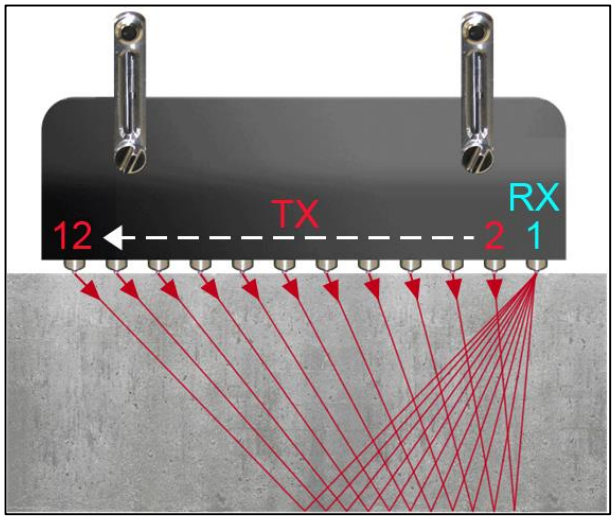

Fig. 2: data acquisition sequence

Parameter	Value	Units
sampling rate	1	MHz
A/D conversion resolution:	14	bits
analog gain	0 to 60	dB
pulse frequency (square wave):	25-85	kHz
pause between pulses:	0 to 50	ms
pulse duration	0.5 to 2	periods
number of measuring blocks	12	
interval between blocks	30	mm

Tab. 1: main characteristics of Tomograph A1040 MIRA

3. SIGNAL COMBINATION AND TOMOGRAM RECONSTRUCTION

As discussed, data acquisition via the ultrasonic tomograph implies collecting a set of 66 waveforms in the time domain (A-scans). This means that any reflector located beneath the sensor array is observed through a number of different emitter-receiver combinations [7]. According to the SAF Technique, in order to consistently combine these signals with reference to a generic point in the resulting tomogram, their amplitude has to be evaluated at the time taken by the incident and the reflected pulses to cover their respective path lengths d_i and d_r (Fig. 3). This is usually performed under the assumption of uniform pulse velocity, whose value is determined by other methods or by calibration at a point of known thickness. A different weight can be assigned to each combined signal based on ray paths angles θ_i and θ_r (apodization factor, taking higher values for smaller angles).

The benefit of coherently merging a number of signals is highlighted in Fig. 4, where the bottom reflection ensuing from an un-grouted tunnel lining segment (thickness = 0.4 m) is detected via both a single A-scan produced by two consecutive sensors and a vertical section of the B-scan obtained through SAFT. In the latter case a definitely lower noise is observed.

The simple combination of signals still preserves the original shape and phase of the diagnostic pulse and allows discerning reflectors of higher or lower acoustic impedance than concrete (grouted or empty post-tensioning duct, Fig. 5). In other applications, a sharper indication of the detected features is preferred, which is allowed by the amplitude envelope of the focused signal. This can be worked out by repeating the focusing procedure on the Hilbert transform of signals, whose phase is shifted by a quarter period

compared to the original waves. The modulus of these two components is representative of the local signal amplitude and allows to cancel the waving aspect of the reflected pulses. This approach was useful, for example, in grouting assessment of a tunnel lining at the soil interface. In such application, the amplitude of the reflected wave was adopted as an indicator of grouting quality. The first two plots in Fig. 6 are the B-scans for well-grouted and un-grouted cases, since the reflection is absent or clearly detectable respectively. By defining some intermediate reflection strengths (4 in the present case), it was possible to categorize the quality of grouting for the tunnel lining, as reported in the map of Fig. 6.

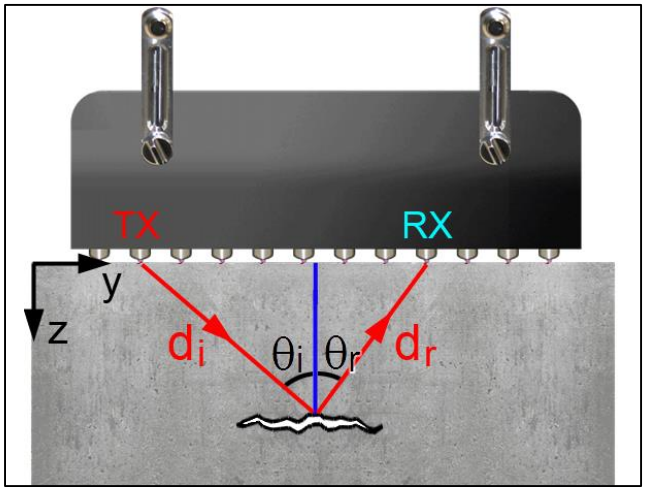

Fig. 3: ray paths at one location in the map

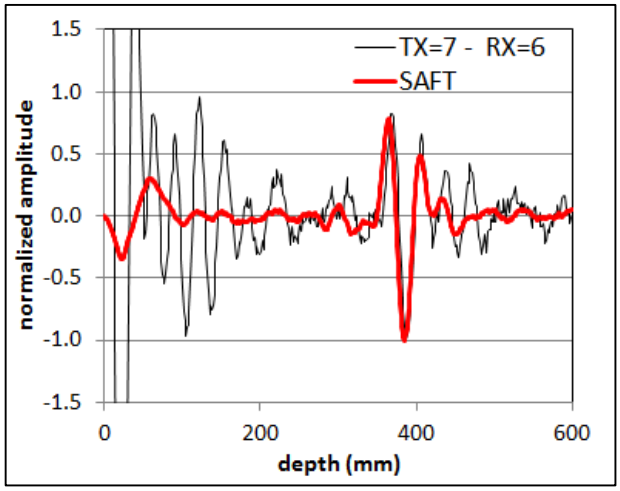

Fig 4: single A-scan vs focused signal

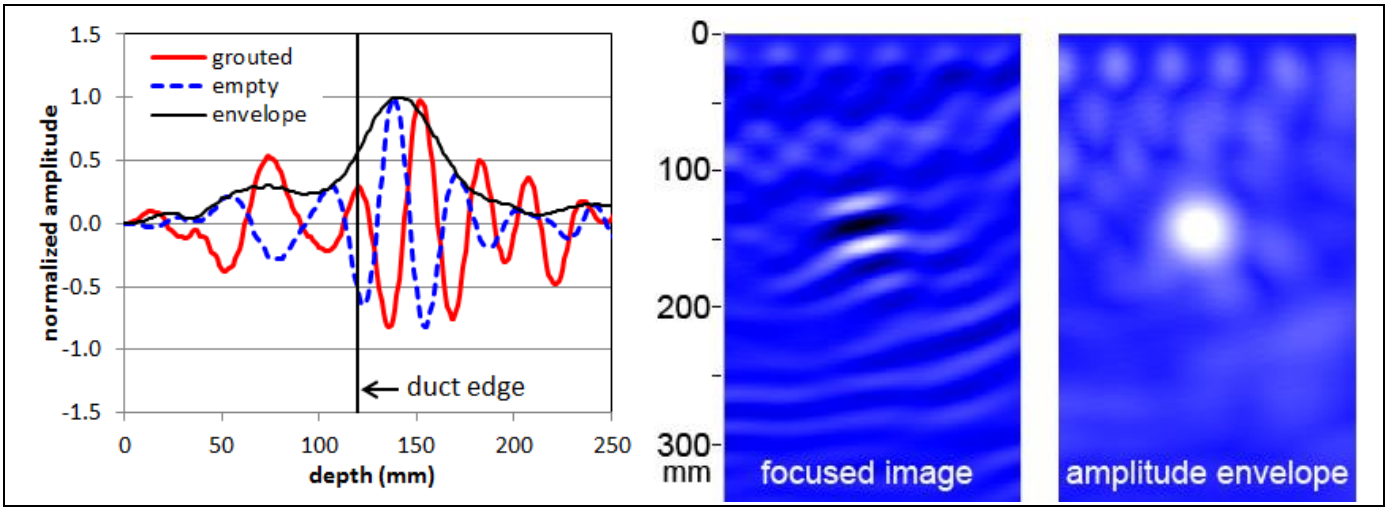

Fig. 5: phase inversion and signal envelope at an empty post-tensioning duct

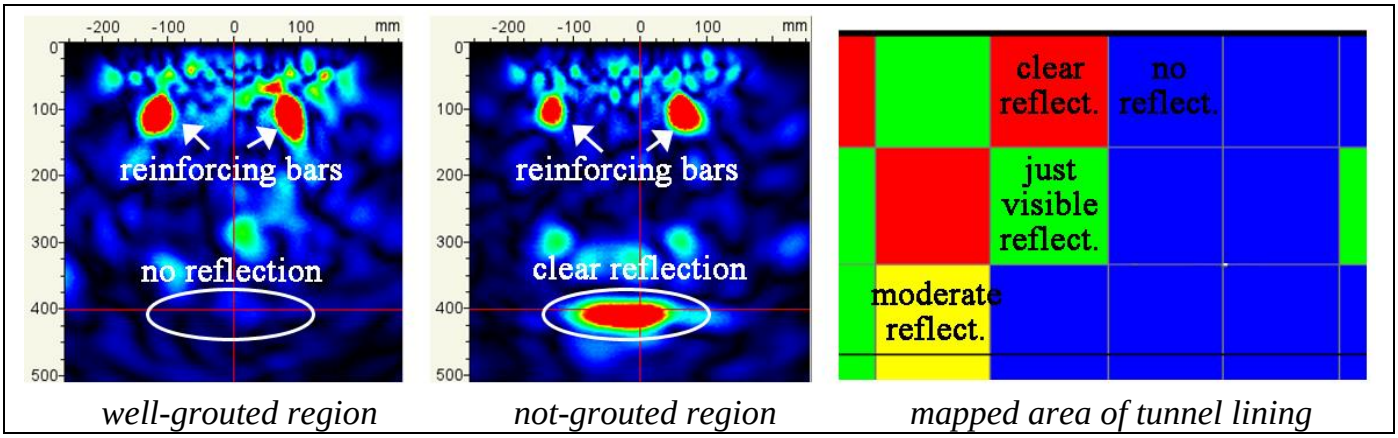

well-grouted region *not-grouted region* *mapped area of tunnel lining*

Fig. 6: grouting assessment in tunnel lining segments

4. WAVES VELOCITY AT THE SURFACE

One accessory information allowed by the A1040 tomograph is the assessment of shear waves velocity, that is the starting point in the implementation of SAFT in elements of unknown material quality. This is made possible by taking advantage of the direct cross-talk among the 12 sensor blocks via waves propagating along the surface. For any emitter-receiver pair, the generated pulse is detected after a time delay depending on their mutual distance and phase velocity (Fig. 7a). By assigning a guess value to this latter, the initial parts of all 66 acquired A-scans can be shifted along the time axis and then summed. The best estimate of phase velocity gives the best overlap among the signals and maximizes the amplitude of the resulting wave, quantified by the envelope peak (Fig. 7b). Since pulses transmitted between farther sensors provide more meaningful information, but they undergo higher attenuation, a weight proportional to the probes distance is assigned in the optimization procedure.

One interesting application of this procedure deals with the assessment of fire damaged concrete elements. Elastic wave velocity at the surface is a very significant damage indicator. Nonetheless, the presence of cracks and the poor efficiency of ordinary probes in the indirect transmission of compressive pulses make the in-situ implementation of traditional UPV rather demanding. On the contrary, shear waves tend to be guided by the damaged layer (Love waves) and undergo less attenuation. Moreover, merging many

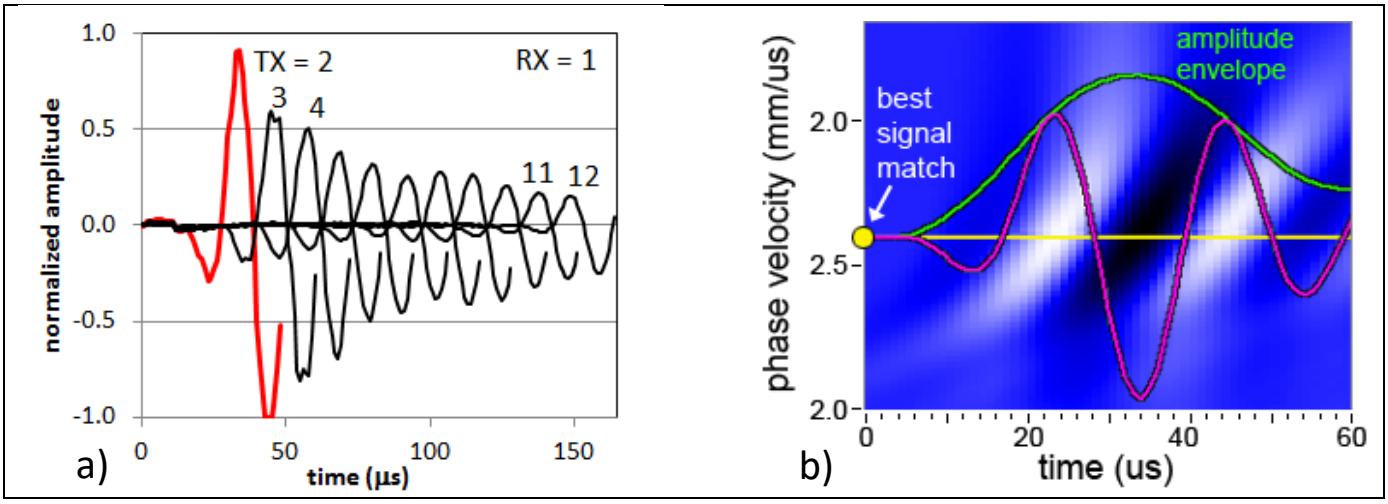

Fig. 7: phase shift at increasing sensor distance and best match of first detected pulses

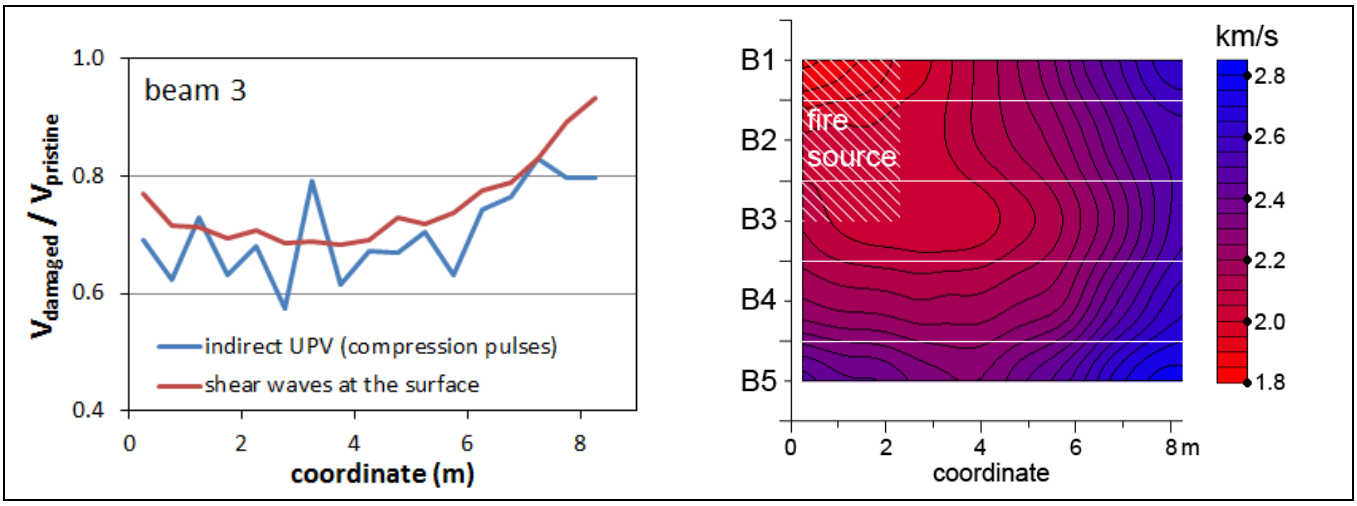

Fig. 8: shear wave velocity at the intrados of a fire damaged concrete overpass

signals acquired in different areas within the sensor array range (330 mm) strongly reduces the impact of possible cracks compared to single indirect UPV measurements.
A pilot case study regards a concrete overpass whose intrados was impacted by the localized fire developed from a burning coach. Results obtained via the tomograph are smoother than traditional indirect UPV (Fig. 8) and a detailed map of the deck conditions could be obtained in a reasonable time (85 points over 80m^2 in 3 hours). Dry coupling of the sensor array allowed by DPC transducer was of considerable help in this application.

5. GUIDED WAVES IN WROUGHT IRON RODS

Another interesting application of the A1040 tomograph is the inspection of historical tie-rods to identify dominant defects. Such flaws usually consist in cracks nucleated along forged welds (the so-called *bolliture*), used in the past to assemble several 1.0-1.5m bars into longer elements. The basic idea is to arrange the A1040 tomograph with the y-axis parallel to the tested element, so to trigger antisimmetric guided waves. This allows also exploiting the advantage brought in by the sensor array, since wrought iron is a heterogeneous material and the combination of many signals via a focusing procedure is expected to enhance the quality of results. Moreover, spring loaded DPC transducers can adapt to the remarkably rough surface and don't require any coupling agent, preserving the original metal from contaminants.
It has to be remarked that the proposed method was developed to address the specific case study of Duomo di Milano, whose rather thick tie-rods (typical cross section 60x90mm) allow good contact with most of sensors in the array. In this application the instrument was used only for raw data acquisition, while post-processing was developed in LabVIEW environment by adapting the method described in [8]. According to this procedure, all pulses travelling along the tie-rod are brought to a common virtual point (e.g. the centre of the array) by shifting them on the time axis according to the distance to the reference point of actual emitters and receivers. The phase velocity required for determining these time shifts is assessed according to the method discussed in the former section, which also produces a picture of the actual diagnostic pulse (see Fig. 7b). The sign assigned to the time shifts allows a separate analyses of pulses travelling in opposite directions.
The aligned signals are then summed and the resulting synthetic wave is examined for detecting any echo reflected by sizable defects. Better indications in terms of signal to noise ratio are obtained by cross correlating the synthetic wave with the diagnostic pulse.
In order to characterize the propagation characteristics of shear waves in tie-rods, the dispersion curves have been calculated (Fig. 9a) by using the semi-analytic method described in [9]. Only some antisimmetric modes (thick coloured lines in the graph) can be triggered and detected by the tomograph, due to the sensitivity to just transverse vibrations (orthogonal to tie-rod axis). The most convenient frequency range for the large section size at issue is between 10 and 20 kHz, since there are only two dominant modes with rather constant velocity. However, due to the operational limits of the tomograph, pulses of frequency not lower than 25kHz and duration of not more than 2 cycles can be generated. This implies a rather broad band of excited frequencies (fig. 9b) which in fact is expected to trigger several highly dispersive modes in Fig. 9a.
The effectiveness of the method has been validated first in laboratory, taking advantage of a highly defective original tie-rod of Duomo di Milano which was replaced several years

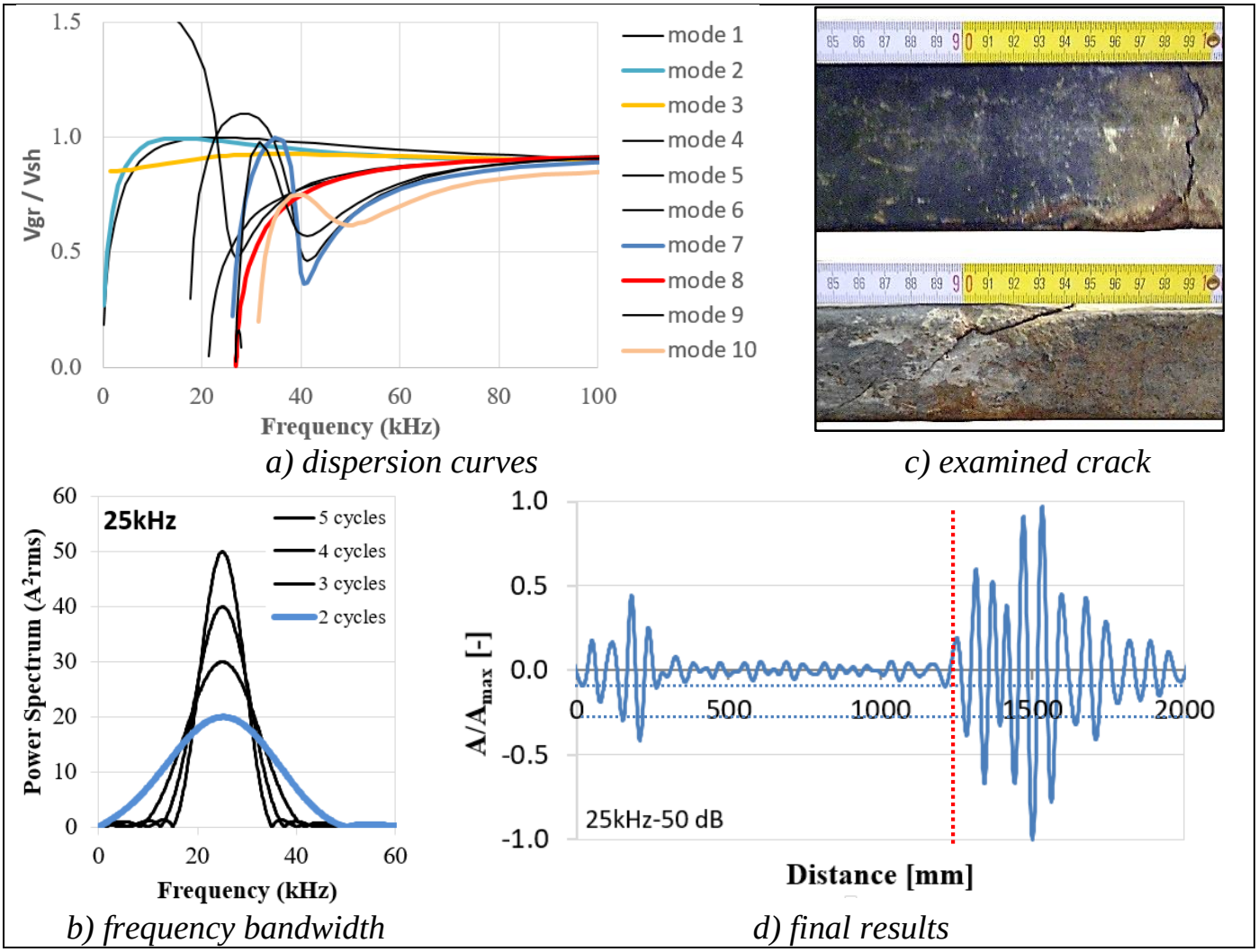

Fig. 9: guided waves in wrought iron rods.

ago. More precisely, it exhibits a deep crack along a forged weld involving about 80% of the tie-rod cross-section with a maximum opening of 1.5 mm (Fig. 9c). Tests have been carried out by coupling the ultrasonic tomograph to one larger vertical side of tie-rod at a distance of about 1.2 m from the known defect. Observing the processed signals (Fig. 9d), a fairly clear indication is visible at the crack location.

The same procedure has been implemented in situ on a smaller crack extending by about 50% of cross section with a maximum opening of 0.3 mm [10]. Although an indication can still be recognized, the influence of noise and dispersion is definitely higher.

6. CONCLUSIONS AND OUTLOOK

In this work the innovative features of A1040 MIRA tomograph have been discussed in order to gain a deeper insight on its working principle and to outline some unconventional applications which may take advantage of the particular structure of this instrument. In general, the option of acquiring in rapid sequence the pulse-echo signals between all possible emitters/receivers combinations within a 12 blocks sensor array allows averaging many observations of the same features in the inspected object. This translates into a significant reduction of the structural noise affecting heterogeneous materials like concrete and wrought iron.

In more details the following additional information have been made available via a proper processing of raw waveform data:

- more detailed analysis of echo phase and amplitude, allowing to categorize the quality and magnitude of interfaces;
- direct assessment of shear wave velocity at the surface of damaged elements;
- identification of main flaws in slender elements like wrought iron tie rods.

Nonetheless, these first promising results call for further developments in different directions. Among them, the robust evaluation of phase and amplitude for structured targets (like post-tensioning ducts), the analysis of pulse refraction in fire damage elements, mode separation and dispersion compensation in guided wave testing.

AKNOWLEDGEMENT

Test methods and case studies discussed in this work lie within the activities of PoliNDT (Inter-Department Lab for Structural Diagnostic and Monitoring) at Politecnico di Milano.

REFERENCES

[1] D.M. McCann and M.C. Forde, “Review of NDT methods in the assessment of concrete and masonry structures”, NDT&E International 34, pp. 71–84, 2001.

[2] M. Schickert, "Ultrasonic NDE of concrete," Proceedings of 2002 IEEE Ultrasonics Symposium, pp. 739-748, 2002. doi: 10.1109/ULTSYM.2002.1193506

[3] P. Shokouhi, J. Wolf and H. Wiggenhauser, “Detection of Delamination in Concrete Bridge Decks by Joint Amplitude and Phase Analysis of Ultrasonic Array Measurements”, ASCE J. Bridge Eng. 19(3), 2014.

[4] M. Krause, B. Milmann, F. Mielentz, D. Streicher, B. Redmer, K. Mayer, K.-J. Langenberg and M. Schickert, “Ultrasonic Imaging Methods for Investigation of Post-tensioned Concrete Structures: A Study of Interfaces at Artificial Grouting Faults and Its Verification”, J Nondestruct. Eval, 27, pp. 67–82, 2008.

[5] M. Schickert, M. Krause and W. Muller, “Ultrasonic Imaging of Concrete Elements Using Reconstruction by Synthetic Aperture Focusing Technique”, ASCE J. Materials in Civil Engineering, pp 235–246, 2003.

[6] K. Mayer, K.-J. Langenberg, M. Krause, B. Milmann and F. Mielentz, “Characterization of Reflector Types by Phase-Sensitive Ultrasonic Data Processing and Imaging”, J Nondestruct Eval, 27, pp. 35–45, 2008.

[7] ORNL. Oak Ridge National Laboratory, “Evaluation of Ultrasonic Techniques on Concrete Structures”, Technical Report ORNL/TM-2013/430, 130 pp., 2013.

[8] S. C. Wooh and Y. Shi, “Synthetic phase tuning of guided waves”, IEEE Trans. on Ultrasonics, Ferroelectrics and Frequency control 48 (1), pp. 209–223, 2001.

[9] J. G. Yu, J. E. Lefebvre, Ch. Zhang and F. E. Ratolojanahary, “Dispersion curves of 2D rods with complex cross-sections: double orthogonal polynomial approach”, Meccanica 50, pp. 109–117, 2015.

[10] M. Bellanova, M. Carboni, R. Felicetti, A. Gianneo, “Individuazione di difetti critici su tiranti storici in ferro battuto”, 17° Congresso AIPnD, Milano, 2017.